Available online at www.sciencedirect.com
ScienceDirect
Physica D 230 (2007) 99–111
PHYSICA D
www.elsevier.com/locate/physd

Exploring the need for localization in ensemble data assimilation using a hierarchical ensemble filter

Jeffrey L. Anderson*

NCAR/Data Assimilation Research Section, P.O. Box 3000, Boulder, CO 80307-3000, United States

Available online 31 July 2006

Abstract

Good performance with small ensemble filters applied to models with many state variables may require 'localizing' the impact of an observation to state variables that are 'close' to the observation. As a step in developing nearly generic ensemble filter assimilation systems, a method to estimate 'localization' functions is presented. Localization is viewed as a means to ameliorate sampling error when small ensembles are used to sample the statistical relation between an observation and a state variable. The impact of spurious sample correlations between an observation and model state variables is estimated using a 'hierarchical ensemble filter', where an ensemble of ensemble filters is used to detect sampling error. Hierarchical filters can adapt to a wide array of ensemble sizes and observational error characteristics with only limited heuristic tuning. Hierarchical filters can allow observations to efficiently impact state variables, even when the notion of 'distance' between the observation and the state variables cannot be easily defined. For instance, defining the distance between an observation of radar reflectivity from a particular radar and beam angle taken at 1133 GMT and a model temperature variable at 700 hPa 60 km north of the radar beam at 1200 GMT is challenging. The hierarchical filter estimates sampling error from a 'group' of ensembles and computes a factor between 0 and 1 to minimize sampling error. An *a priori* notion of distance is not required. Results are shown in both a low-order model and a simple atmospheric GCM. For low-order models, the hierarchical filter produces 'localization' functions that are very similar to those already described in the literature. When observations are more complex or taken at different times from the state specification (in ensemble smoothers for instance), the localization functions become increasingly distinct from those used previously. In the GCM, this complexity reaches a level that suggests that it would be difficult to define efficient localization functions *a priori*. There is a cost trade-off between running hierarchical filters or running a traditional filter with larger ensemble size. Hierarchical filters can be run for short training periods to develop localization statistics that can be used in a traditional ensemble filter to produce high quality assimilations at reasonable cost, even when the relation between observations and state variables is not well-known *a priori*. Additional research is needed to determine if it is ever cost-efficient to run hierarchical filters for large data assimilation problems instead of traditional filters with the corresponding total number of ensemble members.

Keywords: Data assimilation; Ensemble filters; Sampling error; Localization

1. Introduction

Ensemble filter methods for data assimilation in the atmosphere and ocean have been in use for more than a decade. Progressively more powerful and simpler implementations have been applied to a growing array of problems, ranging from low order idealized model studies, through operational atmospheric prediction [1–3].

The Data Assimilation Research Section at NCAR is developing simple, generic assimilation methods for use by scientists with modeling or observational expertise but limited experience with assimilation. Ensemble filters described in the literature still require the specification of model and observation specific parameters for good performance. One common requirement is specifying functions that 'localize' the impact of an observation to a subset of the model state variables, usually a subset that is physically close to the observation [4]. Localization can be essential for small ensemble filters to provide high quality assimilations in large models.

In simple models, for instance univariate low-order models [5], it may be easy to localize the impact of observations. Making a physically motivated assumption that observation impacts should be weighted by a locally supported

* Tel.: +1 303 497 8991; fax: +1 303 497 1700.
E-mail address: jla@ucar.edu.

0167-2789/$ - see front matter © 2006 Elsevier B.V. All rights reserved.
doi:10.1016/j.physd.2006.02.011

Gaussian-like function and tuning the width of this function works very well for many applications. Matters are more complicated in large, multivariate, multidimensional models for atmospheric and oceanic prediction. While many large ensemble filter applications have localized observation impact in the horizontal by a two-dimensional Gaussian-like function, vertical localization has been more challenging [6]. Limiting multivariate impacts, for example the impact of a temperature observation on a wind observation, is also an issue and has received limited study. Observations taken at times different from the model time can also require temporal localization. Questions like: "how should the impact of a radar reflectivity observation from a particular beam angle at 0045 GMT be allowed to impact a model temperature variable located 150 km north of the radar at 300 hPa at 0100 GMT?" [7] need to be addressed in a systematic fashion.

Here, ensemble filtering algorithms are derived as a Monte Carlo approximation to the Bayesian filtering problem [8,9]. Localizing observation impacts on state variables is related to sampling errors in the ensemble filter. A hierarchical Monte Carlo method, in which an ensemble (group) of ensemble assimilations is performed, can estimate these sampling errors. In one-dimensional models, results can be similar to the methods already in use although the new method can estimate the width for Gaussian-like localizations. In large multivariate models, computed localization functions are often non-Gaussian and would be difficult to approximate *a priori*. The hierarchical Monte Carlo method may enhance performance in realistic atmospheric and oceanic assimilation/prediction applications. Short assimilations with a hierarchical filter can be used to provide localization functions for traditional filters for users that are not assimilation or modeling experts. The localization information from the hierarchical filters can then be used to give good performance in small traditional ensembles. Further research is needed to evaluate whether it is ever efficient to use limited computing resources to run a group filter, as opposed to a correspondingly costly larger traditional filter, in real assimilation applications. For now, the hierarchical filters presented here should simply be viewed as a tool for finding appropriate localizations for traditional filter assimilations.

2. Sources of error in ensemble filters

Most key works in the ensemble (Kalman) filtering literature start from the classical Kalman filter [10,11]. Anderson [12] presented an alternative, starting from Bayesian filtering [8] and describing ensemble filtering as the impact of a single observation on a single state variable without loss of generality.

Fig. 1 depicts an ensemble filter implemented in this way. First, a model advances a sample (ensemble) of state estimates from a previous time, t_k, to the time, t_{k+1}, when the next observation is taken (step 1); dashed lines represent model trajectories. A forward operator, H, is applied to each prior state estimate to obtain a prior sample estimate of the observed variable, y (step 2). The observed value, y^o, and observational error distribution (gray density superposed on the y-axis) come from the instrument (step 3). The prior sample and observation

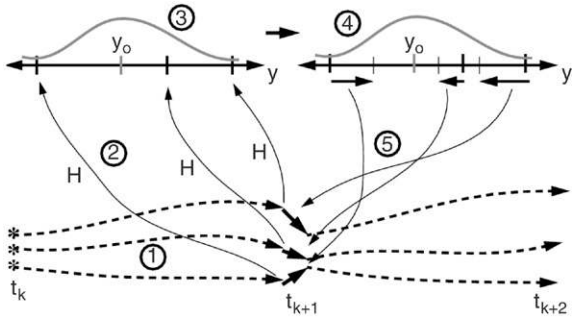

Fig. 1. Schematic representation of the implementation of the ensemble filter used here with possible error sources marked by numbers 1 through 5.

are combined giving an updated sample estimate of y (thin ticks on y-axis) and corresponding increments (vectors below y-axis) (step 4). The details of step 4 distinguish most ensemble (Kalman) filter variants [13–15]. Finally, the prior joint sample of y and a state variable, x_i, are used to compute corresponding increments for each sample of the state variable (vectors at the end of dashed model trajectories at t_{k+1}) (step 5). Usually this is done using linear regression (this is implicit in Kalman filter derivations of ensemble methods). When linear regression is used, each state variable can be updated independently [12] to give a sample of the model state vectors conditioned on the observation.

Errors can be introduced at each step. Model error [16,17], including the fact that model sub-grid scale parameterizations are often not stochastic [18], is introduced in step 1. Forward operators, H, in step 2 are rife with error sources including time and space interpolation errors, representativeness errors, etc. Step 3 introduces errors in retrieving and transmitting observations from instruments and the use of often poorly known instrumental error distributions. Algorithms for step 4 generally approximately model the prior distribution (a Gaussian assumption is most common) and make additional approximations when computing the updated conditional probability. Sampling error from small ensembles is also an issue here. Finally, in step 5 the model-generated relationship between observation and state variables can differ from the relation in the physical system. Errors are also introduced by assuming a linear relation between the observation and state variable increments. Sampling error in linear regression in step 5 can be the dominant source of error in the whole filtering procedure. This paper focuses on ways to minimize this regression sampling error. Sampling error in step 4 can be addressed in a similar fashion but is not addressed here.

3. Dealing with regression error in ensemble filters

There are many ways to deal with sampling errors in the regression step (or observation increment step) of an ensemble filter. The first is to ignore them (and treat results with less confidence). Although simple cases in low order models (Section 5) can work when ignoring sampling error, this approach often fails because filters diverge from the true state of the system.

A second method is to make heuristic assumptions that reduce the confidence given to sample statistics during filter execution. For instance, covariance inflation [19] can alleviate impacts of error from all sources in Section 2 and is predicated on the idea that serious errors in ensemble filters are those that lead to overconfidence in prior estimates. An overconfident prior reduces weight given to subsequent observations leading to further separation of the ensemble from the truth. This can lead to filter divergence where the ensemble estimate is oblivious to observations. Covariance inflation avoids this by increasing the prior variance. After the model is advanced in time (step 1 in Fig. 1), the prior sample variance of each state variable, x_i, is increased by linearly 'inflating' the ensemble around its mean,

$$x_{i,j} = \sqrt{\gamma}\left(x_{i,j} - \bar{x}_j\right) + \bar{x}_j. \tag{1}$$

Here, i indexes the ensemble member, j indexes the state variable element, an overbar is an ensemble mean, and γ is the covariance inflation factor. One can argue that much important information in the prior is retained since inflation leaves the mean and correlations between state variables unchanged [20].

A third method applies physically based assumptions about the underlying prior distribution. Distance dependent localization [21,4] reduces the impact of an observation on a state variable (step 5 in Fig. 1) by a factor that is a function of the 'physical distance' separating them. The compactly supported Gaussian-like fifth order polynomial of Gaspari and Cohn [22], called a GC envelope here, is most commonly used. Another localization used in the literature is the boxcar function used by Anderson and Anderson [20] and found to be inferior to the more smoothly varying GC method. A similar method used by Ott et al. [23] appears to produce good results. Distance dependent localization requires that a 'distance' be defined *a priori* between an observation and each state variable.

A fourth method for dealing with sampling errors makes a statistically based *a priori* estimate of the expected error in the regression coefficient given the numerical model and the set of observations. This appears to be extremely difficult in problems with large non-linear models and complicated forward observation operators.

A fifth method uses *a posteriori* statistical information from a filter to estimate corrections needed for a subsequent assimilation. Assume that sample regression coefficients between an observation taken periodically at a fixed station and all state variables are available from a long *successful* ensemble assimilation. Estimates of the sampling error can be computed under a variety of different assumptions about the underlying 'true' distributions of the coefficients. The sampling error can then be corrected during a subsequent assimilation. In many cases, this method begs the question since an initial successful filter run cannot be made without knowing how to correct for the sampling errors. A related method that is the closest published result to that described here has been used by Houtekamer and Mitchell [24] who split their ensemble into two parts and use statistics from one half to update the other half.

A sixth method uses a Monte Carlo technique to evaluate sampling errors in an ensemble filter. In this study, 'groups' of ensembles are used to understand regression sampling errors in the ensembles.

4. A hierarchical ensemble filter

Assume that m groups of n-member ensembles ($m \times n$ total members) are available. When using linear regression to compute the increment in a state variable, x, given increments for an observation variable, y^o, m sample values of the regression coefficient, β, are available. The regression coefficient for each group is calculated as in a standard ensemble filter as $\beta_i = \sigma_{x,y}/\sigma_{y,y}$ where the numerator is the prior sample covariance of the state variable x and the observed variable y and the denominator is the prior variance of the observed variable both computed using the n members of the ith group. Neglecting other error sources, assume that the correct but unknown value of β is a random draw from the same distribution from which the m samples were drawn. The uncertainty associated with the sample value of β for a given ensemble implies that increments computed for the state variable are also uncertain. A regression confidence (weighting) factor, α, is defined to minimize the expected RMS difference between the increment in a state variable and the increment that would be used if the 'correct' regression factor were used. α is chosen to minimize

$$\sqrt{\sum_{j=1}^{m}\sum_{i=1,i\neq j}^{m}\left(\alpha\beta_i - \beta_j\right)^2} \tag{2}$$

where β_i is the regression factor from the ith group. This is equivalent to finding the α that minimizes

$$\sum_{j=1}^{m}\sum_{i=1,i\neq j}^{m}(\alpha^2\beta_i^2 - 2\alpha\beta_i\beta_j + \beta_j^2). \tag{3}$$

Taking a derivative with respect to α and seeking a minimum gives

$$2\alpha\sum_{j=1}^{m}\sum_{i=1,i\neq j}^{m}\beta_i^2 - 2\sum_{j=1}^{m}\sum_{i=1,i\neq j}^{m}\beta_i\beta_j = 0. \tag{4}$$

The first sum in Eq. (4) can be rewritten as

$$(m-1)\sum_{i=1}^{m}\beta_i^2 \tag{5}$$

and the second sum as

$$\left(\sum_{i=1}^{m}\beta_i\right)^2 - \sum_{i=1}^{m}\left(\beta_i^2\right) \tag{6}$$

so that

$$\alpha_{\min} = \left\{\left[\left(\sum_{i=1}^{m}\beta_i\right)^2 \Big/ \sum_{i=1}^{m}\beta_i^2\right] - 1\right\} \Big/ (m-1). \tag{7}$$

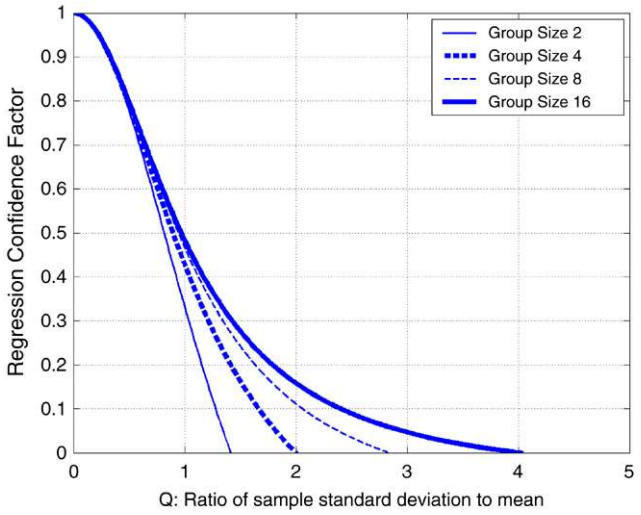

Fig. 2. Regression confidence factors as a function of the ratio Q of regression sample standard deviation to the absolute value of the sample mean for 2 (thin solid), 4 (thick dashed), 8 (thin dashed) and 16 (thick solid) groups.

$\alpha_{\min}$ can be computed directly from Eq. (7) as a function of the sample values β. It can also be written as a function of the ratio, Q, of the sample standard deviation to the absolute value of the sample mean of β

$$\alpha_{\min} = \max\left[\frac{m - Q^2}{(m-1)Q^2 + m}, 0\right]. \tag{8}$$

Fig. 2 plots $\alpha_{\min}$, referred to as a regression confidence factor (RCF), as a function of the ratio Q for group sizes 2, 4, 8 and 16; if $\alpha_{\min}$ is less than zero it is set to zero. Smaller groups have smaller RCFs, especially on the tail of the distribution. When uncertainty is large (larger Q), small groups cannot distinguish signal from noise and the observation is not allowed to impact the state variable.

The hierarchical ensemble filter proceeds as follows. Each n-member ensemble is treated exactly as described in Section 2 except for step 5, the regression computation. A regression coefficient, β_i, $i = 1, \ldots, m$ is computed for each of the m ensembles and the sample mean and standard deviation are computed, along with the ratio Q; the RCF is computed from Eq. (8). The regression is completed for each ensemble using its sample regression coefficient multiplied by the RCF. The set of RCFs for a given observation and the set of model state variables is called a 'regression confidence envelope'. The envelope can be viewed as a localization. Applying a hierarchical filter may also reduce the covariance inflation required for a given assimilation since part of the regression error is often corrected by inflation.

The hierarchical approach is analogous to turbulence closure schemes [25]. Like these, the hierarchical technique must be 'closed' at some level. Here, a second level scheme in which 'groups' of ensembles are used is applied. A 'closure' is obtained by dealing with sampling error in the groups using some other method. This makes sense only if the sampling error at level two is less severe than that from just using one of the other methods in Section 3 for a single ensemble.

5. Regression confidence envelopes in the L96 model

5.1. Experimental design

The 40-variable model of Lorenz (Appendix) [5] is configured with 40 state variables equally spaced on a unit periodic one-dimensional domain. This L96 model has an attractor dimension of 13 [26]. A free integration of the model and prescribed observational error are used to generate synthetic observations to be assimilated by the same model. Forty randomly located 'observing stations' are used in most experiments and observations are available every model time step. The 40 stations are marked by asterisks at the top of Fig. 4a. Forward observation operators, H, are linear interpolations from the nearest model state variables while observational errors are Gaussian with mean 0 and observation error variance varying between 10^{-7} and 10^{7} for different experiments. It is not necessary to assume that the model state is defined at the observing station locations. The stations simply define the forward observation operators.

As noted in Section 2, ensemble filters variants are distinguished by the algorithm used to compute the observation variable increments in step 4. Here, the deterministic square root filter [27] referred to as an Ensemble Adjustment Kalman Filter (EAKF) in Anderson [19] is used. Most results do not change qualitatively when using other observation space update methods such as the classical ensemble Kalman filter [10] or some more exotic techniques [12].

For efficient application of hierarchical filters small group sizes must produce good results. Group sizes of 2, 4, 8 and 16 have been evaluated and comparisons for different group sizes are examined in selected cases.

All hierarchical filter assimilations start with ensemble members selected from a 'climatological' distribution of the L96 model generated by integrating slightly perturbed states for 100,000 time steps. 4000-step assimilations are performed, the first 2000 steps are discarded and results shown from the second 2000 steps. A covariance inflation factor (selected from the set 1.0, 1.0025, 1.005, 1.0075, 1.01, 1.015, 1.02, 1.025, 1.03, 1.04, 1.06, 1.07, 1.08, 1.09, and 1.10 to 1.40 by intervals of 0.02) is tuned by experimentation to give the smallest time mean RMS error for the ensemble mean prior estimate over the final 2000 steps. Initial conditions for the second 2000 steps from the first group of the hierarchical ensemble filter are used as initial conditions for additional single filter assimilations discussed below.

RCF values are kept for each observation/state variable pair at each assimilation time and the time mean and median are computed from the last 2000 steps. Additional assimilation experiments are performed using a single ensemble filter with the same ensemble size. The time mean (median) values of RCFs from the hierarchical filter multiply the regression factors for each observation/state variable pair from the single ensemble; these are referred to as time mean and time median filter assimilations. The covariance inflation factor for the time mean and median cases is selected so that it minimizes the time

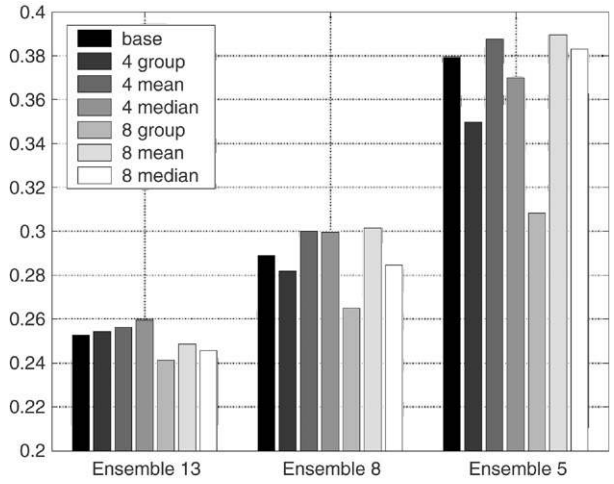

Fig. 3. 2000-step time mean RMS error (normalized by the observational error standard deviation) for observational error variance of 10^{-7} with 13, 8 and 5 member ensembles for standard Gaspari–Cohn localized (base) filter, four group filter and corresponding time mean and time median filter, and eight group filter and corresponding time mean and median filter.

mean RMS error of the ensemble mean over the 2000 steps of the single ensemble assimilation.

In addition, traditional ensemble filters with localization using a GC function are performed for each hierarchical filter case. The optimal value of the GC half-width is selected by searching from the set of values 0.025, 0.05, 0.075, 0.10, 0.125, 0.15, 0.20, 0.25, 0.30, 0.40, 0.50, 0.6, 0.75, 1.0 and 10^8 for that value producing the smallest time mean RMS error over the 2000 steps of the experiment. For each GC half-width the optimal value of the covariance inflation is determined as for the other filters. Results from the combination of GC half-width and covariance inflation that minimizes the RMS are presented.

Time mean values of the RMS error of the prior ensemble mean state variables are used as a rough measure of performance. The time mean of the RMS difference between ensemble members and the ensemble mean (a measure of the ensemble spread) is also computed. In ideal situations, error and spread values should be statistically indistinguishable. For most cases discussed here, the spread is slightly greater than the RMS error for the cases with the smallest RMS error (see Tables 1–5).

5.2. Small observational error results

Initially, tiny observational error variances of 10^{-7} are prescribed. Table 1 includes RMS error and spread values along with optimal values of the covariance inflation factor and GC localization half-width (for the standard filter cases) for a variety of ensemble and group sizes. Fig. 3 compares time mean RMS errors for a variety of filters for ensemble sizes of 13, 8 and 5.

Results for any ensemble size $n > 13$ combined with any number of groups are nearly identical after long assimilations (for small groups, this may be much longer than the standard 2000 steps). Time median RCFs are 1.0 for nearly all observation/state variable pairs and means are greater than 0.99.

Table 1
Comparative RMS error and spread for assimilations with 40 randomly located observations with 10^{-7} error variance for ensemble sizes >13, 13, 8 and 5 and for four-group and eight-group filters with corresponding time mean and time median filters and a traditional filter with Gaspari–Cohn localization (base)

Ensemble size	Group size and type	GC Half-width	Covariance inflation	Time mean RMS error	Time mean spread
>13	Four groups	None	None	0.2335	0.2481
13	8 groups	None	1.04	0.2412	0.2903
	Mean	None	1.03	0.2487	0.2837
	Median	None	1.03	0.2456	0.2748
	Four groups	None	1.04	0.2544	0.2950
	Mean	None	1.03	0.2562	0.2877
	Median	None	1.03	0.2596	0.2838
	Base	0.5	1.04	0.2527	0.2851
8	8 groups	None	1.04	0.2651	0.3297
	Mean	None	1.05	0.3017	0.3145
	Median	None	1.05	0.2845	0.3171
	Four groups	None	1.05	0.2830	0.3274
	Mean	None	1.07	0.3003	0.3523
	Median	None	1.05	0.2996	0.3308
	Base	0.3	1.06	0.2890	0.3113
5	8 groups	None	1.10	0.3084	0.4114
	Mean	None	1.16	0.3895	0.4637
	Median	None	1.14	0.3830	0.4872
	Four groups	None	1.12	0.3497	0.4392
	Mean	None	1.16	0.3877	0.4723
	Median	None	1.07	0.3698	0.4007
	Base	0.15	1.12	0.3792	0.4332
3	8 groups	None	1.24	0.6395	0.8450
	Mean	None	1.28	0.5965	0.7755
	Median	None	Any	Diverges	
	Four groups	None	1.30	0.9075	1.208
	Mean	None	1.28	0.7235	0.9566
	Median	None	Any	Diverges	
	Base	0.1	1.36	0.7595	0.8155

Error and spread values are normalized by the observational error standard deviation.

This indicates that the m ensembles have converged to nearly identical sample covariance estimates. With such tiny error variances, all error sources outlined in Section 2 are so small that sampling error for both the regression and the observation increment becomes negligible. Since all m samples of the regression factor are nearly the same, the true value is known nearly exactly. There is no need for the traditional distance dependent localization.

While sample covariances for $n > 13$ converge to the same values, the sample covariance from any sub-sample of an ensemble does not converge. This is why the hierarchical ensemble filter technique requires independent ensembles rather than partitioning a single large ensemble when computing RCFs.

For $n < 14$, the mean and median RCFs become increasingly localized. Fig. 4a, b shows mean (median) RCFs for the observation at 0.6424, about 70% of the way between

Table 2
Comparative RMS error and spread for assimilations with 40 randomly located observations with various error variances

Observation error variance	Ensemble size	Group size and type	GC half-width	Covariance inflation	Time mean RMS error	Time mean spread
1e–5	14	Four groups	None	1.02	0.2258	0.2564
	14	Mean	None	1.03	0.2380	0.2693
	14	Median	None	1.05	0.2472	0.2928
	14	Base	None	1.03	0.2478	0.2713
	56	Base	None	1.005	0.2153	0.2348
1e–3	14	Four groups	None	1.02	0.2314	0.2584
	14	Mean	None	1.03	0.2352	0.2721
	14	Median	None	1.02	0.2252	0.2528
	14	Base	0.4	1.03	0.2486	0.2800
	56	Base	None	1.0075	0.2177	0.2372
0.1	14	Four groups	None	1.02	0.2488	0.2776
	14	Mean	None	1.04	0.2692	0.3113
	14	Median	None	1.03	0.2630	0.2931
	14	Base	0.3	1.03	0.2657	0.2952
	56	Base	None	1.01	0.2396	0.2575
1.0	14	Four groups	None	1.03	0.2901	0.3230
	14	Mean	None	1.03	0.3121	0.3377
	14	Median	None	1.05	0.3146	0.3652
	14	Base	0.3	1.05	0.3080	0.3426
	56	Base	0.5	1.01	0.2816	0.2885
10.0	14	Four groups	None	1.05	0.3782	0.4294
	14	Mean	None	1.05	0.4052	0.4482
	14	Median	None	1.04	0.4075	0.4502
	14	Base	0.2	1.06	0.4285	0.4245
	56	Base	0.25	1.02	0.3560	0.3712
1e7	14	Four groups	None	None	23.21*	23.02*

14-member ensembles are used for four-group and eight-group filters with corresponding time mean and time median filters. Traditional filters (base) for ensemble sizes of 14 and 56 are also included. Error and spread values are normalized by the observational error standard deviation.

Table 3
Comparative RMS error and spread for assimilations with 40 randomly located observations with 1.0 error variance for ensemble size 14 for 2, 4, 8 and 16 groups with corresponding time mean and time median filters and a traditional filter with Gaspari–Cohn localization (base)

Group size and type	GC half-width	Covariance inflation	Time mean RMS error	Time mean spread
2 groups	None	1.05	0.3066	0.3505
Mean	None	1.06	0.3243	0.3980
Median	None	1.05	0.3297	0.3787
Four groups	None	1.03	0.2901	0.3230
Mean	None	1.03	0.3122	0.3377
Median	None	1.05	0.3146	0.3652
8 groups	None	1.03	0.2854	0.3346
Mean	None	1.04	0.3150	0.3550
Median	None	1.05	0.3096	0.3640
16 groups	None	1.03	0.2795	0.3210
Mean	None	1.04	0.3080	0.3523
Median	None	1.03	0.3042	0.3414
Base	0.3	1.05	0.3080	0.3426

state variables 26 and 27, and all 40 state variables. For $n = 13$, the maximum of the median is 1.0 for state variables 26, 27 and 28 and the minimum is about 0.12 for state variables farthest from the observation. The mean peaks just below 1 and has a minimum of about 0.25. Reducing n to 8 and 5 leads to progressively more localization. The median still has a maximum near 1 for state variable 27, but non-zero values are

Table 4
Comparative RMS error and spread for assimilations with 40 observations located as in Fig. 4 to form a data dense and data void region with 1.0 error variance for 14 member ensembles

Group size and type	GC half-width	Covariance inflation	Time mean RMS error	Time mean spread
Four groups	None	1.015	12.75	13.33
Mean	None	1.03	13.33	13.55
Median	None	1.01	13.59	14.32
Base	0.2	1.02	13.77	13.86

Table 5
Comparative RMS error and spread for assimilations with 40 randomly located observations with forward observation operators being the average of 15-point observations surrounding the central location (for instance at locations $0.6424 + 0.025k$, where $k = -7, -6, \ldots, 6, 7$)

Group size and type	GC half-width	Covariance inflation	Time mean RMS error	Time mean spread
Four groups	None	1.12	2.030	2.797
Mean	None	1.14	2.182	3.116
Median	None	1.12	2.508	3.159
Base	Any	Any	Diverged	

The observational error variance is 4.0 and the mid-points of the 40 observation locations are the same as marked in Fig. 4a.

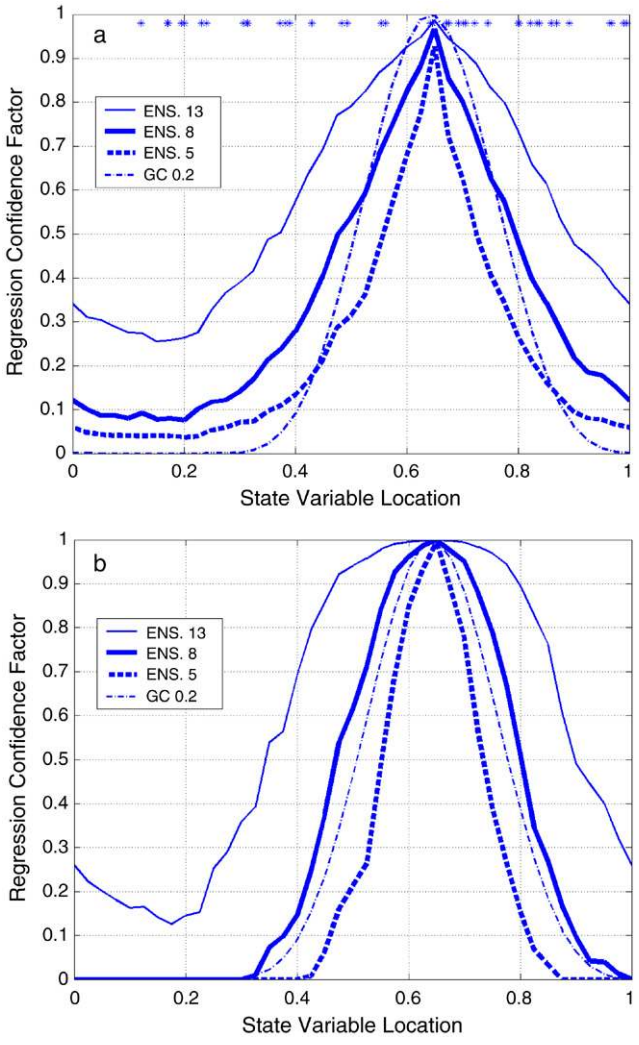

Fig. 4. 2000-step time mean (a) and time median (b) regression confidence factors for Lorenz-96 model assimilations for an observation located at 0.6424 and all 40 state variables. The asterisks at the top of (a) indicate the position of 40 randomly located observations with observational error variance of 10^{-7}. Results are from hierarchical ensemble filters with four groups and ensemble sizes of 5 (thick dashed), 8 (thick solid) and 13 (thin solid). Also shown is a Gaspari–Cohn localization function for a half-width of 0.2 (thin dash–dotted).

confined progressively closer to the observation. The maximum time mean decreases and the RCF is increasingly sharply localized but does not go to 0 far from the observation.

Fig. 3 and Table 1 show that time mean RMS error and spread increase as n is reduced for all methods (hierarchical, time mean, time median, standard). The optimal GC half-width for the traditional filter becomes smaller as n decreases (Table 1), consistent with the time mean and median RCFs.

For $n < 14$, the sample covariance cannot represent the actual covariance because the L96 attractor is on a 13 dimensional manifold. Attempts to apply a traditional filter without localization with $n < 14$ eventually lead to filter divergence. For the hierarchical filter, errors due to this type of degeneracy can be characterized as noise. Smaller ensembles have larger errors in computing β and the corresponding RCFs are smaller (Fig. 4).

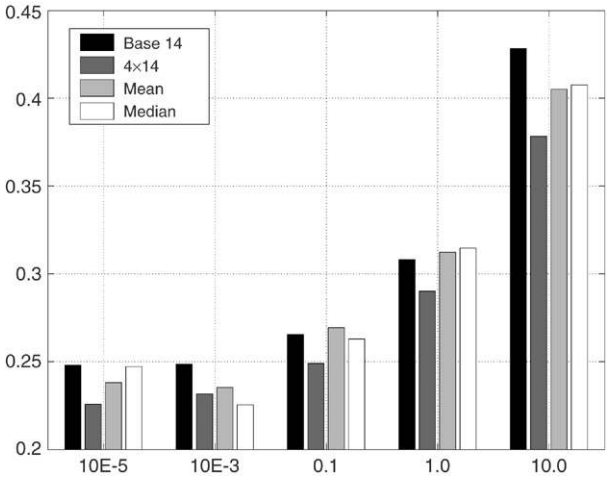

Fig. 5. 2000-step time mean RMS error (normalized by the observational error standard deviation) for observational error variances of 10^{-5}, 10^{-3}, 0.01, 1.0 and 10.0 for standard Gaspari–Cohn localized filter (base 14), four-group filter and corresponding time mean and time median filters, all with ensemble size 14.

There is remarkable similarity between the time mean/median RCF envelopes and the GC function. The GC localization with half-width 0.2 is displayed in Fig. 4a, b; this is between the optimal half-widths of 0.3 for eight ensemble members and 0.15 for five ensemble members. The central portion of the GC is similar in shape to the time median RCFs in Fig. 4b. The RCF envelopes produced from 2000-step assimilations display evidence of sampling noise making them appear less smooth than the GC functions. Noise in the time mean and median RCFs is one factor that leads the time mean and median ensemble filters to produce RMS errors that are often slightly larger than those from the optimal GC traditional filter (Figs. 3, 5 and 7; Tables 1–5).

5.3. Varying observational error variance

Noise can also be introduced into the assimilations by decreasing the number of observations, decreasing the frequency of observations, or increasing the observational error variance. Here, the observational error variance is increased.

Fig. 6a, b show the time mean (median) RCFs as the observational error variance is increased to 10^{-5}, 10^{-3}, 0.1, 1.0, 10.0 and 10^{7}. Table 2 shows the error, spread, and parameter settings for filters applied in these problems while Fig. 5 compares the time mean RMS errors. Results are for four groups and $n = 14$. As the error variance increases the response of the RCF envelopes is similar to that from reducing the ensemble size. Larger error variance leads to more compact median RCFs and more strongly peaked means. The case with error variance 10^{7} has prior ensembles with climatological distributions since the observations have negligible impact (so there is no point in comparing error results from different types of filters). The RCF envelopes in this case have an interesting double peaked structure. When beginning an assimilation from a climatological distribution (a safe and simple choice in many cases), this approximates the appropriate localization.

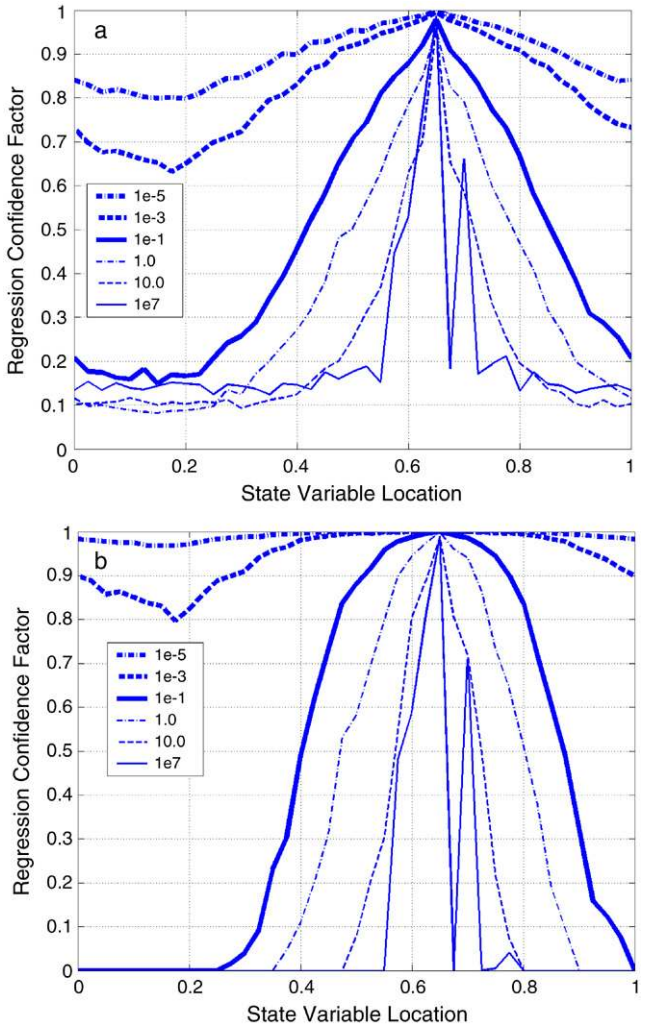

Fig. 6. 2000-step time mean (a) and time median (b) regression confidence factors for Lorenz-96 model assimilations for an observation located at 0.6424 and all 40 state variables. Results are from hierarchical ensemble filters with four groups and 14 ensemble members. The observational error variance for 40 randomly located observations is 10^{-5} (thick dash–dotted), 10^{-3} (thick dashed), 10^{-1} (thick solid), 1.0 (thin dash–dotted), 10.0 (thin dashed) and 10^{7} (thin solid).

Sampling error introduced into the regression by reducing the information available from the observations is qualitatively similar to that from degenerate ensembles (Section 5.2). While gaining an understanding of these two sources of error may require independent analysis, the hierarchical filter approach addresses both types of errors.

An advantage of the hierarchical filter is that it does not require tuning of a localization function like the GC half-width. Heuristic tuning can require many iterations, even in one dimensional, univariate models like L96 with simple forward observation operators. Tuning of localization becomes much more difficult in multivariate three-dimensional models with complex forward observation operators.

5.4. Impact of group size on results

Fig. 7 shows RMS errors for different group sizes for the 40 random observation, 1.0 error variance case with $n = 14$ while

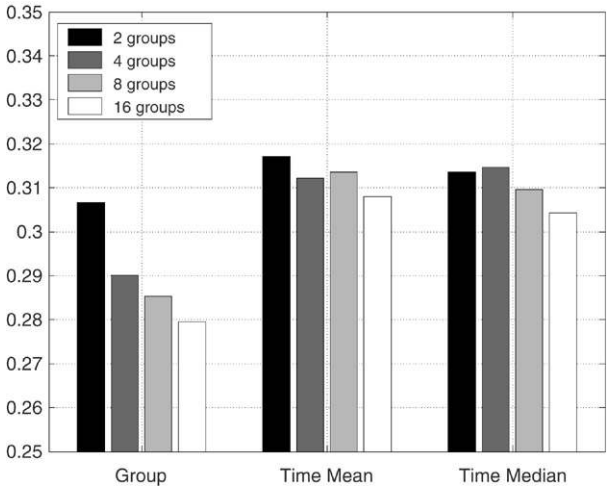

Fig. 7. 2000-step time mean RMS error (normalized by the observational error standard deviation) for observational error variance of 1.0 and hierarchical filters with group sizes of 2, 4, 8 and 16 along with the corresponding time mean and time median filters.

Table 3 shows details on these assimilations. Increasing group size leads to a gradual reduction of error. The corresponding time mean and median filters show this behavior to a lesser extent. Fig. 8a, b show the time mean (median) RCFs for group sizes 2, 4, 8 and 16. Close to the observation, group size has almost no impact. Larger differences are seen in the tails where increasing group size leads to progressively smaller values of the RCF. This reflects sampling error in the groups (second level sampling error) in the hierarchical filter. Time mean error decreases with group size (Table 3). With large enough models, hierarchical filters can have the same type of sampling problems as traditional filters, only at level two. The most straightforward way to address this second level sampling error is to include a heuristic localization (like GC) in concert with the hierarchical filter.

5.5. Time variation of regression confidence factors

Fig. 9a, b show RCFs from steps 1000 to 1050 for the 1.0 observational error variance case with $n = 14$ for groups of 16 (2). The time mean (median) of the full 2000 steps can be seen in Fig. 6a, b. Close to the observation, the median (Fig. 6b) indicates that the RCF is usually close to 1. However, Fig. 9a, b depict occasions when the value is small, for instance near time 1033. The group 2 results (Fig. 9b) are noisier, with many significantly non-zero values for state variables remote from the observation. The relative lack of non-zero values for $m = 16$ suggests that much of the non-zero time mean RCF far from the observation is related to second order sampling error.

6. Regression confidence factors for different observation types

6.1. Spatially inhomogeneous observations

Fig. 10 shows 40 observation locations characterizing a well-observed and a poorly observed region in the L96 model. 39

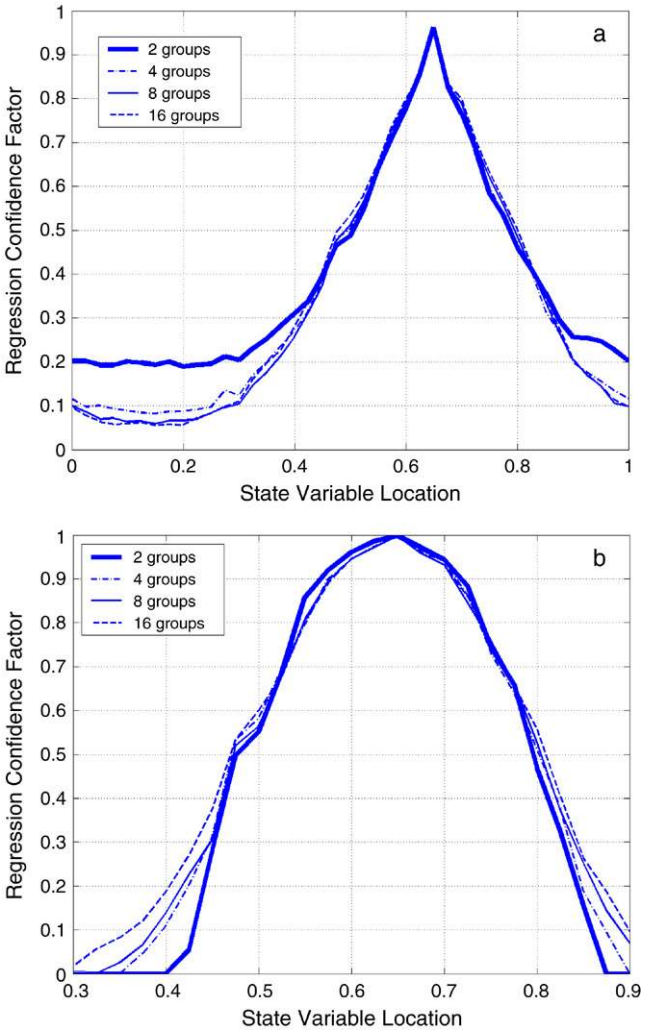

Fig. 8. 2000-step time mean (a) and time median (b) regression confidence factors for Lorenz-96 model assimilations for an observation located at 0.6424 and all 40 state variables. The observational error variance for 40 randomly located observations was 1.0. Results are for 2 groups (thick solid), 4 groups (thin dash–dotted), 8 groups (thin solid) and 16 groups (thin dashed) of 14-member ensembles.

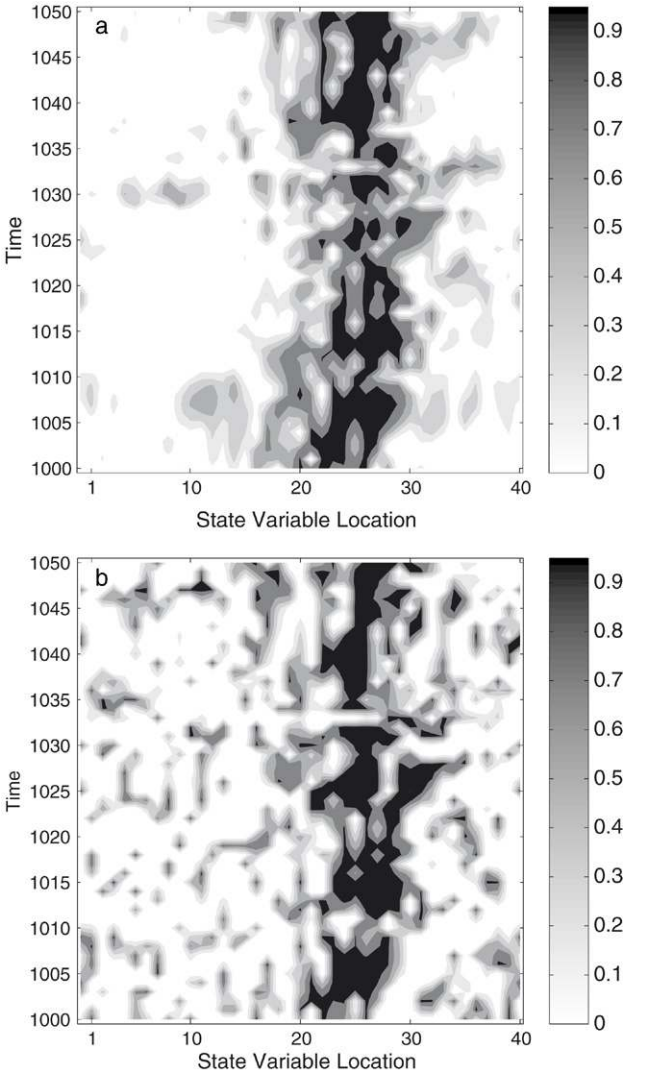

Fig. 9. Regression confidence factor for Lorenz-96 model assimilations for an observation located at 0.6424 and all 40 state variables as a function of time between assimilation steps 1000 and 1050 of a 16 group (a) and 2 group (b) hierarchical filter with ensemble size of 14. The contour interval is 0.2 with values greater than 0.2 shaded and values greater than the added contour 0.95 shaded black.

observations are equally spaced between 0.011 and 0.391 while the 40th observation is located at 0.701. All observations have an error variance of 1.0. The RMS error of three assimilations as a function of state variable is also plotted. In the data dense region, there is no visible difference between the error characteristics of a standard filter, an $m = 4$ filter, and its corresponding time mean filter, all with $n = 14$. However, in the data sparse region, the hierarchical filter and the time mean filter show reduced time mean error (see also Table 4).

Fig. 11a, b show the mean (median) RCF envelopes for observations at 0.011, 0.191, 0.391, and 0.701. RCF envelopes for the observation at 0.191 are relatively wide consistent with low error cases from the previous section. Observations located in larger time mean error areas away from the center of the densely observed region have progressively narrower RCF envelopes. The RCF for the observation at 0.701 is very narrow and displays the two-lobed structure found for very large errors in the previous section. The observation at 0.011, immediately downstream of the poorly observed region, has intermediate width but a triply peaked structure not seen in previous examples.

The optimized GC half-width for the traditional filter is 0.2, relatively broad compared to the RCFs in data sparse regions. The result is that the standard filter performs well in the data dense region but has increased RMS error along with reduced spread in poorly sampled regions.

Atmospheric and oceanic prediction problems continue to present significant disparities in observation spatial density. Hierarchical filters could deal with these areas, but traditional filters would require spatially varying localizations. Effects of temporal variations in observation density are similar and may also be significant for real assimilation problems. Traditional data is denser at 00Z and 12Z in the atmosphere while many remote sensing observations are only available during certain orbital periods or under certain atmospheric conditions. A

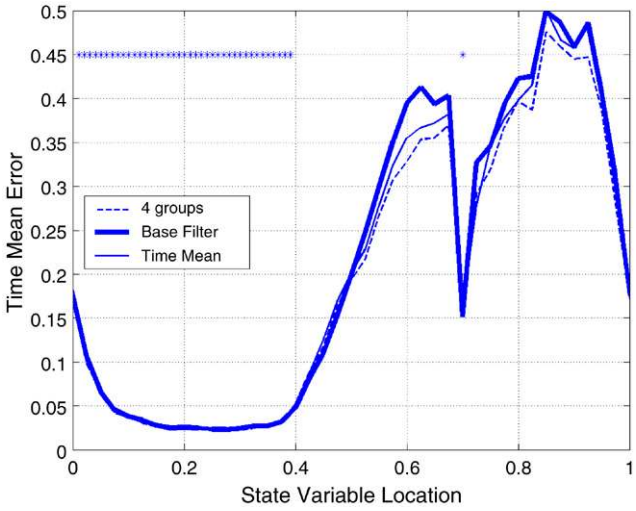

Fig. 10. 2000-step time mean RMS error as a function of model state variable for 14 member ensemble assimilations of 40 observations with observational error variance of 1.0 whose location is indicated by the asterisks at the top of the plot. Results are plotted for a four-group hierarchical filter (thin dashed), a filter using the time mean regression confidence factors from the four-group filter (thin solid), and a traditional ensemble filter (base) with a Gaspari–Cohn localization with half-width 0.2.

hierarchical filter might perform better than a standard filter or a time mean/time median filter since it may be able to resolve time-varying components of the sampling error.

6.2. *Spatially averaged observations*

Satellite observations measuring the total amount of water vapor in an atmospheric column are used in many operational assimilation systems. Other satellite observations have fields of view that are not small compared to the spacing of model gridpoints (especially in the vertical). Forward operators for these observations must be viewed as a weighted average of a large number of model variables.

Spatially averaged observations are simulated in the L96 model by defining a forward observation operator that averages a 0.375 wide domain of the state variables. Given an observation located at x_o, this operator averages 15 standard forward observation operators located at $x_o + 0.025k$, where $k = -7, -6, \ldots, 6, 7$. The 40 observing stations from Section 5.1 are used with error variance of 4.0. Filters with $n = 14$ are used.

Fig. 12 shows the time mean and median RCF envelopes for the observation at 0.6424. Both have a broad maximum with values around 0.6 centered on the observation. The median has an abrupt drop to 0 near the edge of the averaging region while the mean decreases more gradually to a minimum of about 0.15.

Table 5 shows the time mean error results for a $m = 4$ hierarchical filter, its time mean and time median, and a standard filter. Relatively large values of covariance inflation were required, suggesting that the level of sampling error in this problem is larger than in previous examples. The standard filter diverged for all pairs of GC localization half-widths and covariance inflation. If an $n = 14$ standard filter with GC

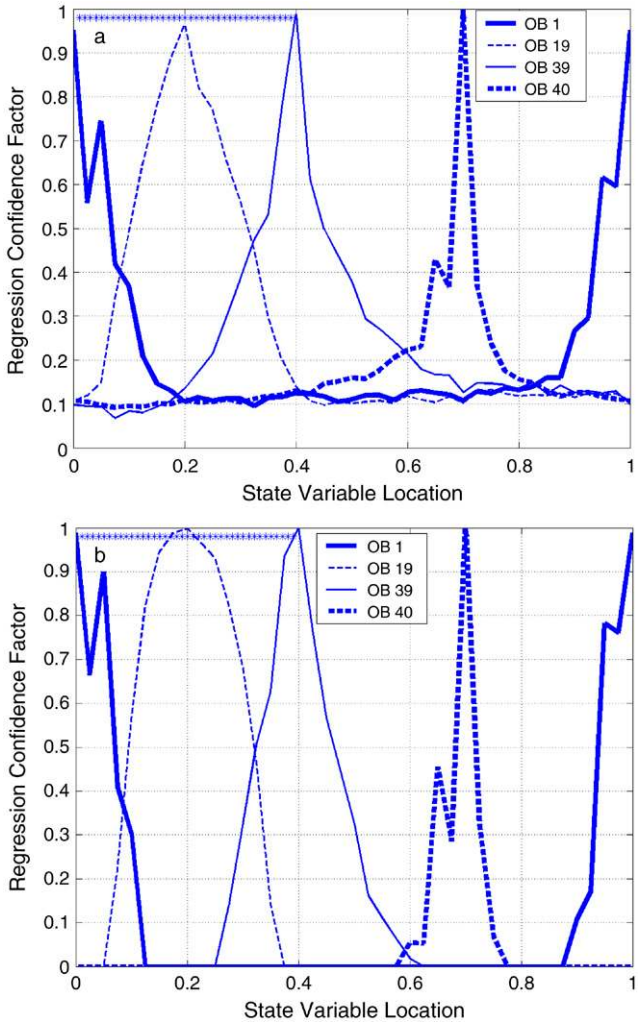

Fig. 11. 2000-step time mean (a) and time median (b) regression confidence factors for Lorenz-96 model four-group hierarchical filter with 14-member ensembles. The observations are as for Fig. 10 and the locations are marked with asterisks at the top of the plot. Regression confidence factors are plotted for the observation at location 0.011 (thick solid), 0.191 (thin dashed), 0.391 (thin solid) and 0.701 (thick dashed).

localization that works for this problem exists, it would work only for a very narrow range of parameters. On the other hand, the $m = 4$ hierarchical filter produced roughly similar RMS error for a range of covariance inflation.

Causes of the standard filter's problem are apparent. The GC functions are defined so that state variables close to the observation location receive the full impact of the observation. The standard filter increments for a given state variable and a relatively small GC half-width are too heavily influenced by a group of close observations and insufficiently influenced by more distant observations. The local over-weighting can be corrected by large covariance inflation, but only by sacrificing even more of the information from more distant observations. Observations for which the forward operators involve averaging in time or combinations of spatial and temporal averaging should also prove challenging with *a priori* localization.

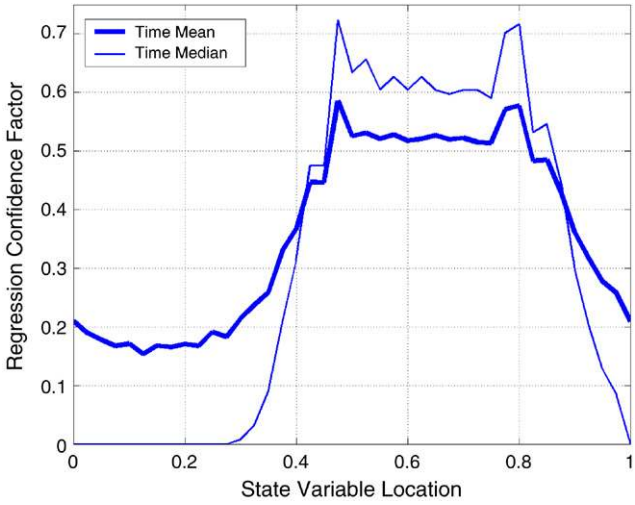

Fig. 12. 2000-step time mean (thick) and time median (thin) regression confidence factors for Lorenz-96 model assimilations with a four-group 14-member ensemble filter for an observation located at 0.6424 and all 40 state variables. The forward observation operators are the average of 15-point observations surrounding the central location (for instance at locations $0.6424+0.025k$, where $k = -7, -6, \ldots, 6, 7$). The observational error variance is 4.0 and the mid-points of the 40 observation locations are the same as marked in Fig. 4a.

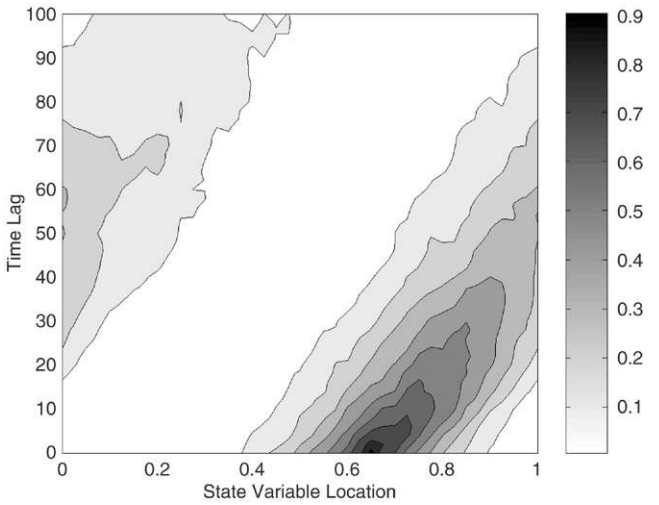

Fig. 13. 1000-step time mean regression confidence factors for simulated time-lagged observation at location 0.6424 for assimilations with a four-group 14-member hierarchical ensemble filter. The base observation set is the 40 random observations as marked in Fig. 4a with error variance 1.0. The plot shows the regression confidence factors for an observation that was taken 'time lag' assimilation steps prior to the time at which it was assimilated. The contour interval is 0.1.

7. Assimilation of observations from different times

As observations become increasingly 'distant' from the state estimate in time, one expects sampling noise to become an increasingly large problem [28]. This is examined using an $m = 4$, $n = 14$ hierarchical filter. The observations in Section 5.1 with observational error variance 1.0 are used. In addition, a single late arriving observation, located at 0.6424, is available from a previous time. The time lag between when this observation was taken and when it is available for assimilation is varied from 0 to 100 assimilation times in a series of 101 experiments. The forward observation operator is applied to the state at the time the delayed observation was taken and archived until the time at which it is assimilated.

Fig. 13 shows the time mean RCF envelopes for the delayed observation as a function of the lag time. For short lag times, a horizontal cross section through Fig. 13 looks very similar to the thick solid curve in Fig. 6a; that experiment differs only in not having an additional lagged observation available. As the lag increases, the RCF maximum shifts downstream and is gradually reduced. This reflects the advection of 'information' by the model from the observation location. The amplitude decrease reflects increasing noise in the sample regressions between the lagged observation and the state as the expected relationship becomes weaker.

There is interest in the development of ensemble smoothers that use observations both from the past and the future to develop an accurate analysis of the state of the system [29]. Appropriate localization in time would be crucial in smoother applications. A plot of the impact of a future observation at location 0.6424 as a function of lag would look very similar to Fig. 13 reflected around a vertical line at 0.6424.

Ensembles are a natural tool for targeted observation experiments [30,31]. These experiments assume that there exist certain observations whose deployment can be controlled [32]. Normally, there is some delay involved in deploying targeted observations. Hence, targeted observation experiments normally involve using forecasts initiated at time t_0 to determine the deployment of observations at time $t_0 + t_{\text{tar}}$ in order to improve some forecast element at time $t_0 + t_{\text{ver}}$, which is even further in the future [33,34].

The reduction in expected spread for the function of the state variables at time $t_0 + t_{\text{ver}}$ can be computed by regressing the expected reduction in the spread of the ensemble estimate of an observation at time $t_0 + t_{\text{tar}}$ onto the verification quantity using the ensemble sample joint distribution of the potential targeted observation and the function at the verification time. This regression will be subject to sampling noise [35] which would require localization in time and space.

8. Estimating non-local model parameters

The use of assimilation to obtain estimates of model parameters has been discussed in the literature [36]. Anderson [19] used assimilation in the L96 model to obtain the value of the parameter F found in Eq. (A1). Localization in ensemble filters requires addressing the question "what is the distance between the parameter and an observation at a given location?"; a hierarchical filter is a natural way to answer this.

A modified version of the L96 model in which the forcing parameter, F, is treated as a 41st model variable is used for a hierarchical filter assimilation. F is fixed at 8.0 in the control integration that generates synthetic observations. Observation locations are the same as in Section 5.1 with an observational error variance of 1.0. An $m = 4$, $n = 14$ filter has an RMS error of 1.714 with spread 1.868. The time mean RMS

error in the estimate of F is 0.01212 (initial values for F are randomly selected from U [7,9]). Time mean values of the RCF between individual observations and F vary between 0.18 and 0.24 implying that F is weakly influenced by any single observation. This is not surprising since F impacts the state globally while the observations are correlated only with a local portion of the state. It is intriguing that this experiment gives the lowest RMS error for the 40 standard state variables of any case examined although all other cases know F exactly. Apparently the uncertainty introduced into the prior estimates by the varying values of F corrects for other sources of error.

9. PE dynamical core on a sphere

Most simple examples of assimilation in the L96 model result in RCF envelopes that are approximately Gaussian. It is difficult for hierarchical group filters to perform better than the best heuristically tuned GC localized filters in these cases. More complicated, multivariate models in higher dimensions might produce less Gaussian RCFs that provide additional motivation for using hierarchical ensemble filters for assimilation. Here, the dynamical core of the GFDL B-grid climate model is used to do a preliminary exploration of this issue.

The B-grid core [37,38] is configured in one of the lowest resolutions that supports baroclinic instability in a Held-Suarez configuration [39] with a 30 latitude by 60 longitude grid and five vertical levels. Assimilation with traditional ensemble filters has been explored in this model in Anderson et al. [38].

1800 randomly located surface pressure stations are fixed on the surface of the sphere and provide observations every 12 h with error standard deviation of 1 hPa. This set of observations can constrain not only the surface pressure field, but also the rest of the model variables.

Assimilations are performed over a 100-day period, starting with ensemble members drawn from a climatological distribution. Results here are for a $m = 4$, $n = 20$ hierarchical filter with no covariance inflation.

Fig. 14 shows the RCFs for a surface pressure observation at 22.7N 61.4E with surface pressure state variables while Fig. 15 shows the RCFs for the same observation with the v wind field at model levels 2 to 5. The RCFs, especially for v, are not well described by Gaussians, with multi-modal structures being apparent. The v RCFs do not have maxima near 1.0 at any level. The structure in the vertical is also non-Gaussian with a minimum at the middle levels. The vertical structure of the RCF in experiments with realistic GCMs (for instance NCAR's CAM3.0) is even more complex and suggests that vertical correlation errors may be a major source of error in traditional ensemble filters. It is important to note that the B-grid model RCFs are even more complex than indicated in Figs. 14 and 15 because they vary considerably depending on the latitude of the observation.

10. Discussion and conclusions

Given ensembles of state variable assimilation results from a successful assimilation and a description of the observing

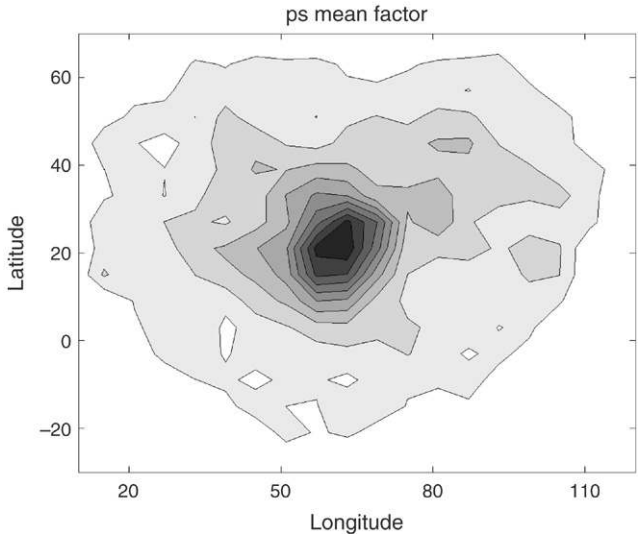

Fig. 14. Time mean regression confidence factor for a pressure observation at 22.7N 61.4E and surface pressure state variables in the GFDL B-grid AGCM. Contour interval is 0.1.

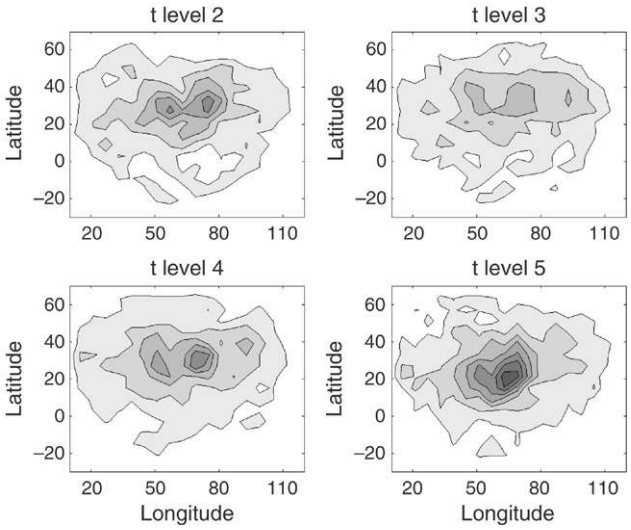

Fig. 15. Time mean regression confidence factors for the same surface pressure observation as in Fig. 14 but with v at each of the model levels 2 through 5. Contour interval is 0.1.

system, it is possible to approximate the RCFs without using a group filter. Knowing the underlying distribution of the correlation between an observation and a state variable allows the computation of the expected time mean RCF. However, in order to compute the RCF in this way, one needs a successful assimilation that in turn requires a high-quality localization of observation impact or a very large ensemble to reduce sampling error. The hierarchical ensemble filter presented here provides a mechanism for producing high quality assimilations with less *a priori* information about how the impact of observations on state variables should be localized. Instead, a Monte Carlo technique is applied to limit the impacts of ensemble sampling error. This technique can deal with situations in which the appropriate 'localization' of the impact of an observation on

a state variable is a complicated function of both observation type, state variable type, spatial location of both the observation and the state variables, and time.

In the low order L96 results that comprise most of this report, the performance of hierarchical filters and traditional ensemble filters that use a prescribed localization is roughly equivalent. However, the traditional ensemble filters require many experiments to tune. In addition, when starting from climatological distributions (which is perhaps the safest way to design assimilation experiments of this sort) the traditional ensemble filter may not be able to deal with the initial phases of the assimilation with large prior error spread while still providing high quality assimilations once the initial error is reduced. A hierarchical filter application is required to provide initial conditions for the traditional ensemble filter in such cases.

In complex multivariate models like atmospheric prediction models, *a priori* specification of localization functions becomes problematic. Even the appropriate distance between spatially and temporally collocated observations and state variables becomes unclear when the observation and state are of different types. When the added complexity of non-local forward operators, vertical and horizontal separation, and temporal separation are considered, the problem becomes very complex indeed. Matters are only made worse by the fact that ensemble size and error size also come into play. While naively localized ensemble filters have produced decent results in large multivariate models, it appears likely that performance could be enhanced by applying hierarchical filters.

Cost, of course, is an important consideration. While results from even small numbers of groups appear to lead to good estimates of sampling error in ensembles, this added expense may be the straw that breaks the camel's back for operational application. However, using short hierarchical experiments to produce statistics for creating localization functions is probably affordable. The resulting ensemble filters using these statistics for localization cost no more than traditional ensemble filters. Hopefully, addressing sampling error and other error sources in ensemble filters will continue to make them even more competitive with other existing assimilation methods and easier for non-experts to apply.

Appendix. The Lorenz-96 model

The L96 [5] model has N state variables, $X_1, X_2, \ldots, X_N$, and is governed by the equation

$$\mathrm{d}X_i/\mathrm{d}t = (X_{i+1} - X_{i-2})X_{i-1} - X_i + F, \tag{A1}$$

where $i = 1, \ldots, N$ with cyclic indices. Here, N is 40, $F = 8.0$, and a fourth-order Runge–Kutta time step with $\mathrm{d}t = 0.05$ is applied as in Lorenz and Emanuel [26].

References

[1] A.C. Lorenc, Quart. J. Roy. Meteor. Soc. 129 (2003) 3183.
[2] C.L. Keppenne, M.M. Rienecker, Mon. Weather Rev. 130 (2002) 2951.
[3] P.L. Houtekamer, H.L. Mitchell, G. Pellerin, M. Buehner, M. Charron, L. Spacek, B. Hansen, Mon. Weather Rev. 133 (2005) 604.
[4] T.M. Hamill, J.S. Whitaker, C. Snyder, Mon. Weather Rev. 129 (2001) 2776.
[5] E.N. Lorenz, ECMWF Seminar on Predictability, Vol. I, ECMWF, Reading, United Kingdom, 1996, 1. pp.
[6] H.L. Mitchell, P.L. Houtekamer, G. Pellerin, Mon. Weather Rev. 130 (2002) 2791.
[7] C. Snyder, F. Zhang, Mon. Weather Rev. 131 (2003) 1663.
[8] A.H. Jazwinski, Stochastic Processes and Filtering Theory, Academic Press, 1970, 376 pp.
[9] A. Tarantola, Inverse Problem Theory, Elsevier Science, 1987, 613 pp.
[10] G. Evensen, J. Geophys. Res. 99 (C5) (1994) 10143.
[11] R.E. Kalman, Trans. AMSE J. Basic Eng. 82D (1960) 35.
[12] J.L. Anderson, Mon. Weather Rev. 131 (2003) 634.
[13] P.L. Houtekamer, H.L. Mitchell, Mon. Weather Rev. 126 (1998) 796.
[14] J.S. Whitaker, T.M. Hamill, Mon. Weather Rev. 130 (2002) 1913.
[15] D.T. Pham, Mon. Weather Rev. 129 (2001) 1194.
[16] D.P. Dee, R. Todling, Mon. Weather Rev. 128 (2000) 3268.
[17] J.A. Hansen, Mon. Weather Rev. 130 (2002) 2373.
[18] R. Buizza, M. Miller, T.N. Palmer, Quart. J. Roy. Meteor. Soc. 125 (1999) 2887.
[19] J.L. Anderson, Mon. Weather Rev. 129 (2001) 2894.
[20] J.L. Anderson, S.L. Anderson, Mon. Weather Rev. 127 (1999) 2741.
[21] H.L. Mitchell, P.L. Houtekamer, Mon. Weather Rev. 128 (2000) 416.
[22] G. Gaspari, S.E. Cohn, Quart. J. Roy. Meteor. Soc. 125 (1999) 723.
[23] E. Ott, B. Hunt, I. Szunyogh, A. Zimin, E. Kostelich, M. Corazza, E. Kalnay, D. Patil, J. Yorke, Tellus A 56 (2004) 415.
[24] P.L. Houtekamer, H.L. Mitchell, Mon. Weather Rev. 129 (2001) 123.
[25] G.L. Mellor, T. Yamada, Rev. Geophys. Space Phys. 20 (1982) 851.
[26] E.N. Lorenz, K.A. Emanuel, J. Atmospheric Sci. 55 (1998) 399.
[27] M.K. Tippett, J.L. Anderson, C.H. Bishop, T.M. Hamill, J.S. Whitaker, Mon. Weather Rev. 131 (2003) 1485.
[28] S.J. Majumdar, C.H. Bishop, B.J. Etherton, I. Szunyogh, Z. Toth, Quart. J. Roy. Meteor. Soc. 127 (2002) 2803.
[29] Z. Li, M. Navon, Quart. J. Roy. Meteor. Soc. 127 (2001) 661.
[30] C.H. Bishop, B.J. Etherton, S.J. Majumdar, Mon. Weather Rev. 129 (2001) 420.
[31] S.P. Khare, J.L. Anderson, Tellus A 58 (2006) 179.
[32] T. Bergot, G. Hello, A. Joly, S. Malardel, Mon. Weather Rev. 127 (1998) 743.
[33] L.M. Berliner, Z.-Q. Lu, C. Snyder, J. Atmos. Sci. 56 (1999) 2536.
[34] C.A. Reynolds, R. Gelaro, T.N. Palmer, Tellus 52A (2000) 391.
[35] T.M. Hamill, C. Snyder, Mon. Weather Rev. 130 (2001) 1552.
[36] J.C. Derber, Mon. Weather Rev. 117 (1989) 2437.
[37] B.L. Wyman, Mon. Weather Rev. 124 (1996) 102.
[38] J.L. Anderson, B. Wyman, S. Zhang, T. Hoar, J. Atmos. Sci. (2005) 2925.
[39] I.M. Held, M.J. Suarez, Bull. Amer. Meteor. Soc. 75 (1994) 1825.